January 2015

Ridge subduction sparked reorganization of the Pacific plate-mantle system 60-50 million years ago

Maria Seton
University of Sydney

Nicolas Flament
University of Sydney, nflament@uow.edu.au

Joanne Whittaker
University of Tasmania

R Dietmar Muller
University of Sydney

Michael Gurnis
California Institute of Technology

See next page for additional authors

Ridge subduction sparked reorganization of the Pacific plate-mantle system 60-50 million years ago

Abstract

A reorganization centered on the Pacific plate occurred ~53-47 million years ago. A "top-down" plate tectonic mechanism, complete subduction of the Izanagi plate, as opposed to a "bottom-up" mantle flow mechanism, has been proposed as the main driver. Verification based on marine geophysical observations is impossible as most ocean crust recording this event has been subducted. Using a forward modeling approach, which assimilates surface plate velocities and shallow thermal structure of slabs into mantle flow models, we show that complete Izanagi plate subduction and margin-wide slab detachment induced a major change in sub-Pacific mantle flow, from dominantly southward before 60 Ma to north-northeastward after 50 Ma. Our results agree with onshore geology, mantle tomography, and the inferred motion of the Hawaiian hot spot and are consistent with a plate tectonic process driving the rapid plate-mantle reorganization in the Pacific hemisphere between 60 and 50 Ma. This reorganization is reflected in tectonic changes in the Pacific and surrounding ocean basins.

Publication Details

Seton, M., Flament, N., Whittaker, J., Muller, R. Dietmar., Gurnis, M. & Bower, D. J. (2015). Ridge subduction sparked reorganization of the Pacific plate-mantle system 60-50 million years ago. Geophysical Research Letters, 42 (6), 1732-1740.

Authors

Maria Seton, Nicolas Flament, Joanne Whittaker, R Dietmar Muller, Michael Gurnis, and Dan J. Bower

AGU PUBLICATIONS

Geophysical Research Letters

RESEARCH LETTER

10.1002/2015GL063057

Key Points:

- Pacific Eocene reorganization was triggered by a ridge subduction event
- Izanagi plate subduction and slab detachment altered Pacific mantle flow
- Our geodynamic models agree with seismic tomography and onshore geology

Supporting Information:

- Text S1 and Figures S1–S4

Correspondence to:
M. Seton,
maria.seton@sydney.edu.au

Citation:
Seton, M., N. Flament, J. Whittaker, R. D. Müller, M. Gurnis, and D. J. Bower (2015), Ridge subduction sparked reorganization of the Pacific plate-mantle system 60–50 million years ago, *Geophys. Res. Lett.*, *42*, 1732–1740, doi:10.1002/2015GL063057.

Received 6 JAN 2015
Accepted 23 FEB 2015
Accepted article online 24 FEB 2015
Published online 24 MAR 2015

Ridge subduction sparked reorganization of the Pacific plate-mantle system 60–50 million years ago

Maria Seton[1], Nicolas Flament[1], Joanne Whittaker[2], R. Dietmar Müller[1], Michael Gurnis[3], and Dan J. Bower[3]

[1]EarthByte Group, School of Geosciences, University of Sydney, Sydney, New South Wales, Australia, [2]Institute for Marine and Antarctic Studies, University of Tasmania, Hobart, Tasmania, Australia, [3]Seismological Laboratory, California Institute of Technology, Pasadena, California, USA

Abstract A reorganization centered on the Pacific plate occurred ~53–47 million years ago. A "top-down" plate tectonic mechanism, complete subduction of the Izanagi plate, as opposed to a "bottom-up" mantle flow mechanism, has been proposed as the main driver. Verification based on marine geophysical observations is impossible as most ocean crust recording this event has been subducted. Using a forward modeling approach, which assimilates surface plate velocities and shallow thermal structure of slabs into mantle flow models, we show that complete Izanagi plate subduction and margin-wide slab detachment induced a major change in sub-Pacific mantle flow, from dominantly southward before 60 Ma to north-northeastward after 50 Ma. Our results agree with onshore geology, mantle tomography, and the inferred motion of the Hawaiian hot spot and are consistent with a plate tectonic process driving the rapid plate-mantle reorganization in the Pacific hemisphere between 60 and 50 Ma. This reorganization is reflected in tectonic changes in the Pacific and surrounding ocean basins.

1. Introduction

A plate reorganization around the Pacific at approximately 53–47 Ma [*O'Connor et al*., 2013; *Whittaker et al*., 2007] is observed via a range of tectonic events including changes in direction of motion of the Pacific [*Caress et al*., 1988; *Lonsdale*, 1988; *O'Connor et al*., 2013] and Australian [*Whittaker et al*., 2007] plates, a reorganization of the Pacific triple junction [*Cande et al*., 1982], cessation of spreading in the Tasman and Coral Seas [*Gaina et al*., 1998], and initiation of Izu-Bonin [*Ishizuka et al*., 2011] and Tonga-Kermadec [*Bloomer et al*., 1995] subduction (Figure 1). The bend in the Hawaii-Emperor chain has been attributed to this reorganization [*Sharp and Clague*, 2006]; however, recent studies have suggested a more localized event may explain this bend [*Tarduno et al*., 2009]. The geodynamic processes and consequences as well as its ultimate driver (either a plate tectonic [*Whittaker et al*., 2007] or mantle flow mechanism [*Finn et al*., 2005]) remain poorly understood. Plate-driven mechanisms often invoke a readjustment in plate-driving forces, especially at plate margins, such as the spontaneous nucleation of subduction along a fracture zone [*Stern*, 2004], complete subduction of an oceanic plate [*Whittaker et al*., 2007], or continent-continent collision [*Molnar and Tapponnier*, 1975; *Patriat and Achache*, 1984], to explain global plate motion changes. In contrast, mantle-driven mechanisms require sudden changes in mantle flow, predominately influenced by plume interactions, such as plume-ridge capture [*Tarduno et al*., 2009] or the arrival of a plume head [*Cande and Stegman*, 2011], but may also be thought of in terms of mantle overturning events, such as a slab avalanche [*Goes et al*., 2008]. These events, which occur in the mantle, then propagate to changes in plate motions at the surface.

A plate-driven mechanism in the form of subparallel intersection of the Izanagi-Pacific ridge along the East Asia subduction zone between 60 and 50 Ma [*Whittaker et al*., 2007] (Figure 2) has been postulated as the cause of the Eocene Pacific plate reorganization. Although plate reconstructions and island arc geochemistry predict the intersection of a mid-ocean ridge with the East Asian margin some time from the Cretaceous to the Eocene [*Straub et al*., 2009] (Figure 1), the absence of large swaths of Pacific-Izanagi ocean floor and fragmented geochemical, volcanic and heat flow data sets from East Asia make it impossible to verify this plate tectonic scenario using geological and geophysical constraints alone. Instead, we use a method that compares the history of subduction predicted by a coupled plate kinematic-geodynamic model with present-day mantle structure imaged in seismic tomographic inversions. This approach allows us to place constraints on the geodynamic implications of whole-scale detachment of the Izanagi slab and examine the effect of this end-member model on mantle flow in the Pacific hemisphere between ~53 and 47 Ma.

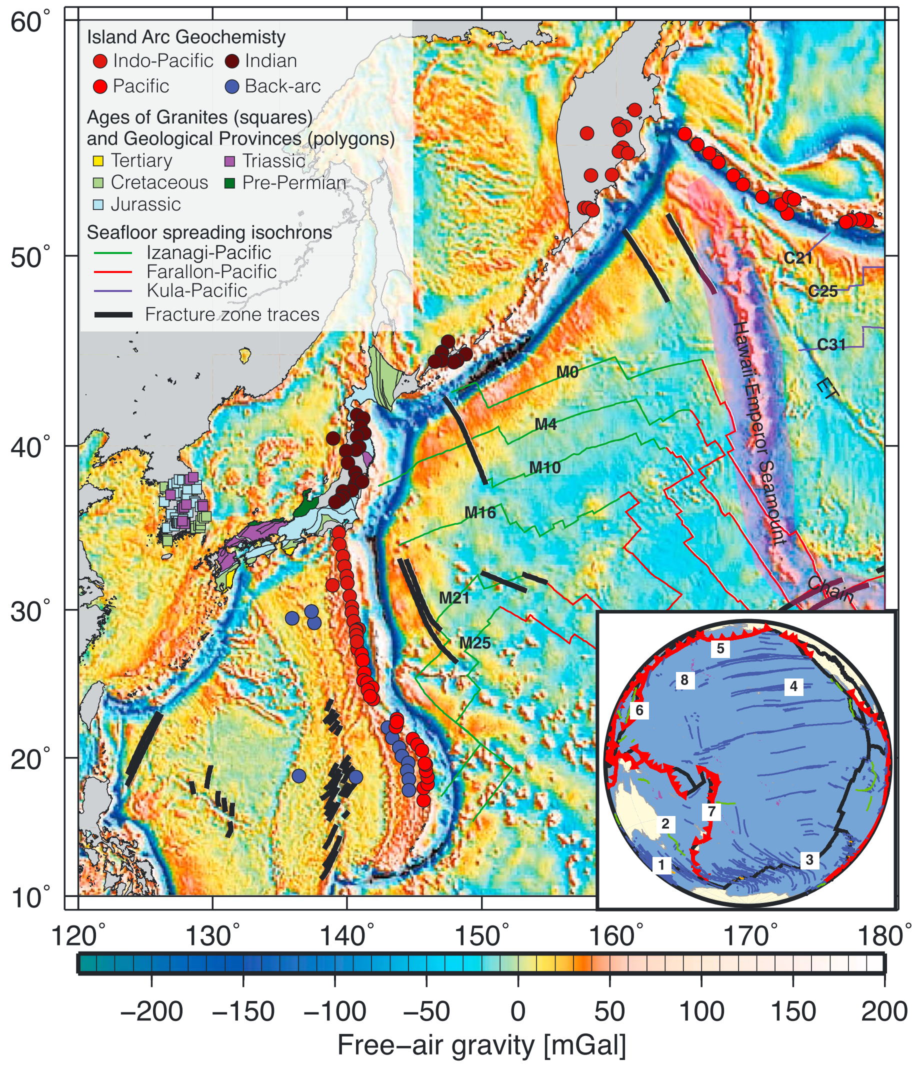

Figure 1. Plate tectonic setting for East Asia and evidence for an Eocene reorganization around the Pacific. Free-air gravity anomalies of the northwest Pacific, with island arc geochemistry [*Straub et al.*, 2009], South Korean granite ages [*Sagong et al.*, 2005], ages of Japanese metamorphic province protoliths [*Nakajima*, 1996], seafloor-spreading isochrons [*Seton et al.*, 2012], and fracture zones traces [*Matthews et al.*, 2011]. Seafloor-spreading isochrons are labeled based on magnetic anomaly chron. The Hawaii-Emperor Seamount Chain is highlighted by a purple polygon. ET = Emperor Trough. Globe insert is centered on the Pacific hemisphere with numbers denoting regions where tectonic events have been mapped: (1) Major change in spreading direction between Australia and Antarctica at chron 21 (~48 Ma) [*Whittaker et al.*, 2007]; (2) cessation of spreading in the Tasman and Coral Seas, east of Australia at ~52 Ma [*Gaina et al.*, 1998]; (3) reorganization of the triple junction in the South Pacific between chrons 22–21 (~50–48 Ma) [*Cande et al.*, 1982]; (4) change in spreading direction between the Farallon and Pacific plates between chrons 24–21 (~53–48 Ma) [*Caress et al.*, 1988]; (5) major change in spreading direction between the Kula and Pacifc plates at chron 24 (~53 Ma) and eventual cessation of spreading at about 41 Ma [*Lonsdale*, 1988]; (6) initiation of arc volcanism along Izu-Bonin-Mariana Arc [*Ishizuka et al.*, 2011]; (7) initiation of subduction along the Tonga-Kermadec Arc [*Bloomer et al.*, 1995]; (8) bend in the Hawaii-Emperor chain starting at 50 Ma [*O'Connor et al.*, 2013; *Sharp and Clague*, 2006]. Red lines indicate subduction zones, black lines transform faults and mid-ocean ridges, blue lines fracture zones, green lines extinct ridges, and purple polygons seamounts and Large Igneous Provinces that erupted between 60 and 40 Ma.

2. Methodology

2.1. Tectonic Reconstructions

We implement an Izanagi plate motion model by reconstructing the now-subducted ocean floor of the Pacific and proto-Pacific/Panthalassa based on the preserved seafloor-spreading record and deriving full-stage rotations by assuming spreading symmetry [*Seton et al.*, 2012] when only one flank of the spreading system is

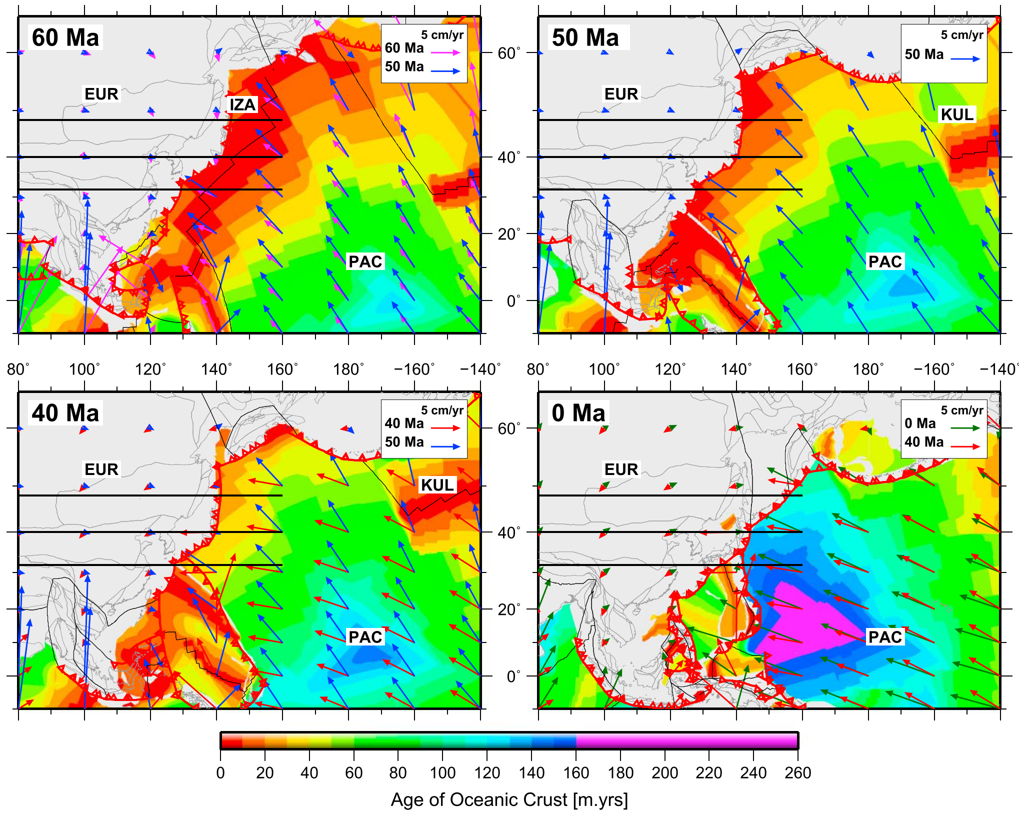

Figure 2. Palaeo-agegrids of the northwest Pacific before (60 Ma), during (50 Ma), and after (40 Ma) the slab break-off event, and at the present day. Absolute plate velocity vectors at 60 Ma (magenta), 50 Ma (blue), 40 Ma (red), and present day (green). Mid-ocean ridges and transforms are plotted as thin black lines, and subduction zones as red lines. Thick black lines denote the location of the profiles used in Figures 4 and S1–S3. EUR = Eurasian plate, IZA = Izanagi plate, KUL = Kula plate, PAC = Pacific plate, and PIR = Pacific-Izanagi Ridge.

preserved or when both flanks are missing. Spreading symmetry is a simple and reasonable assumption since ~95% of all present-day seafloor is characterized by spreading symmetry [*Müller et al.*, 1998]. We construct topological plate polygons with evolving plate boundaries [*Gurnis et al.*, 2012], compute palaeo-age grids, and extract velocity fields in 1 Myr intervals (Figure 2).

2.2. Geodynamic Models

In order to predict the mantle structure implied by the plate reconstruction, we use an approach that links plate tectonic modeling using *GPlates* [*Boyden et al.*, 2011] with spherical mantle convection using the finite-element software *CitcomS* [*Tan et al.*, 2007] by assimilating plate kinematics, the thermal structure of the oceanic lithosphere, and the shallow portion of slabs at 1 Myr increments into forward mantle flow models [*Bower et al.*, 2015].

The incompressible, global mantle flow models start at 230 Ma. The mesh consists of 12 caps, each with 128 × 128 × 64 elements, for a total of ~12.6 million elements and an average lateral resolution of ~ 50 km at the surface and ~ 28 km at the core-mantle boundary. Using vertical mesh refinement, we obtain a radial resolution of 15 km in the surface boundary layer, 27 km in the lower boundary layer, and an average radial resolution of 62 km. The Rayleigh number, defined using the thickness of the mantle, is ~ 7.8×10^7, and internal heat production is neglected. Viscosity varies by 1000 due to temperature dependence following

$$\eta = \eta_0 \times \exp\left(\frac{E_a}{R\Delta T(T + T_\eta)} - \frac{E_a}{R\Delta T(T_b + T_\eta)}\right),$$

where $\eta_0 = 1 \times 10^{21}$ Pa s is the reference viscosity, $E_a \approx 100$ kJ mol^{-1} (upper mantle) or $E_a \approx 33$ kJ mol^{-1} (lower mantle) is the activation energy, $R = 8.31$ J mol^{-1} K^{-1} is the universal gas constant, $\Delta T = 2800$°C is the

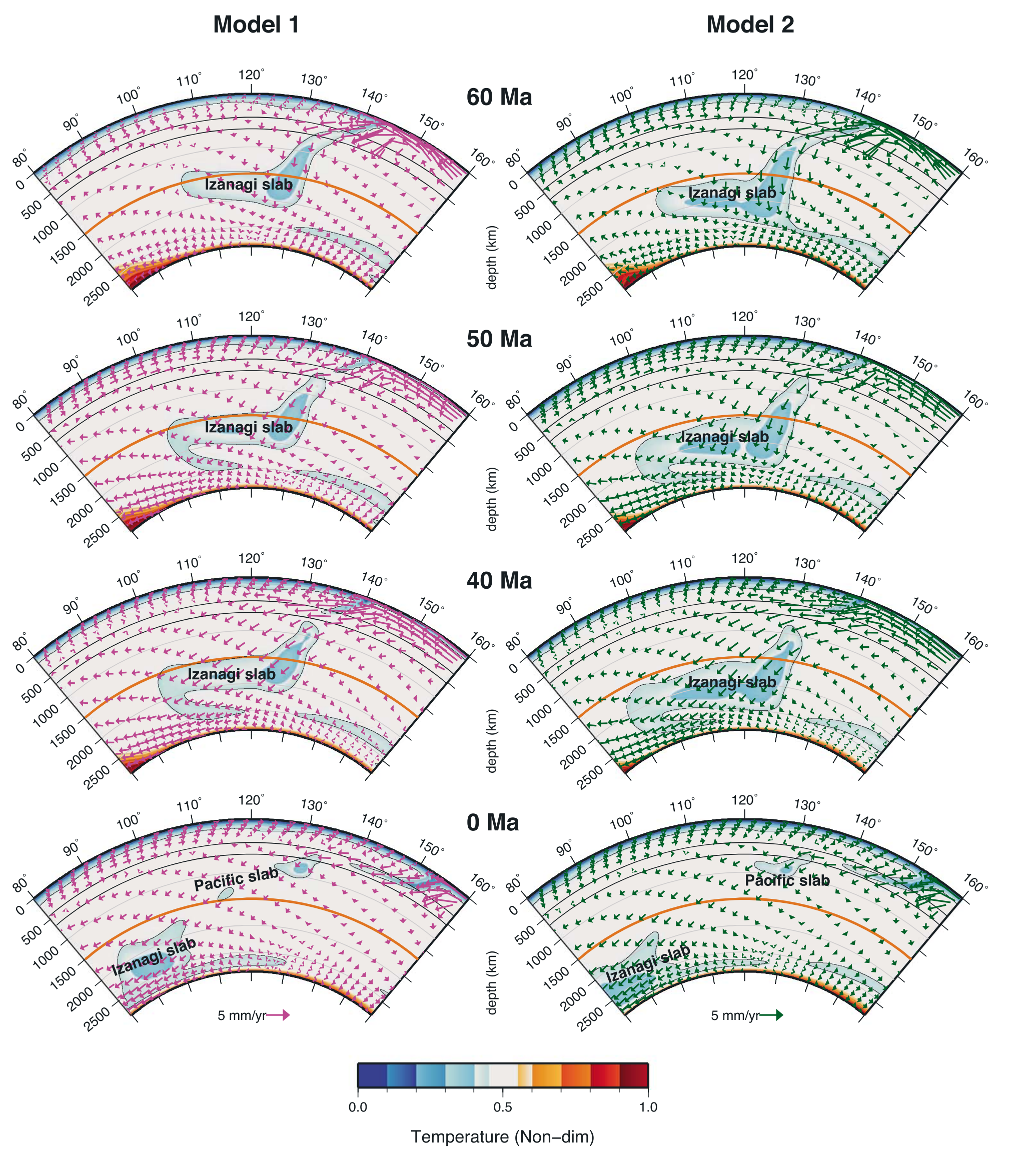

Figure 3. Temperature and velocity fields at 48°N predicted by Models 1 and 2, with kinematic boundary conditions, before (60 Ma), during (50 Ma), and after (40 Ma) the slab break-off event, and at present day. Black contours indicate material 10% colder than the ambient mantle, associated with subducted slabs. Orange line denotes the depth of the map shown in Figures 4 and S1–S3.

temperature drop across the mantle, T is the temperature, $T_\eta \approx 225$°C is a temperature offset, and $T_b = 1400$°C is the ambient mantle temperature.

We present three models that differ in the viscosity of the asthenosphere and of the lower mantle and use Model 1 as reference. In Models 1 and 3, the viscosity of the lower mantle is 100 times greater than that of the upper mantle, and η_0 is reduced by a factor of 10 between 160 and 310 km depth to include the influence of a weak asthenosphere. In Model 3, this asthenosphere is only present under oceans: numerical tracers 10 times more viscous than ambient mantle are used to offset the viscosity drop under the continents. In Model 2, which does not include an asthenosphere, viscosity increases by a factor of 10 at the upper to lower mantle and linearly increases across the lower mantle by a factor of 10 (as in case TC7 of *Flament et al.* [2014]). To inhibit plume development (since our objective is to focus on the effect of subduction), all models include an initially 113 km thick layer 3.6% denser than ambient (with reference to $\rho_0 = 4000\ \mathrm{kg\ m^{-3}}$) at the base of the mantle (as in cases HH1-HH3 of *Flament et al.* [2014]).

10.1002/2015GL063057

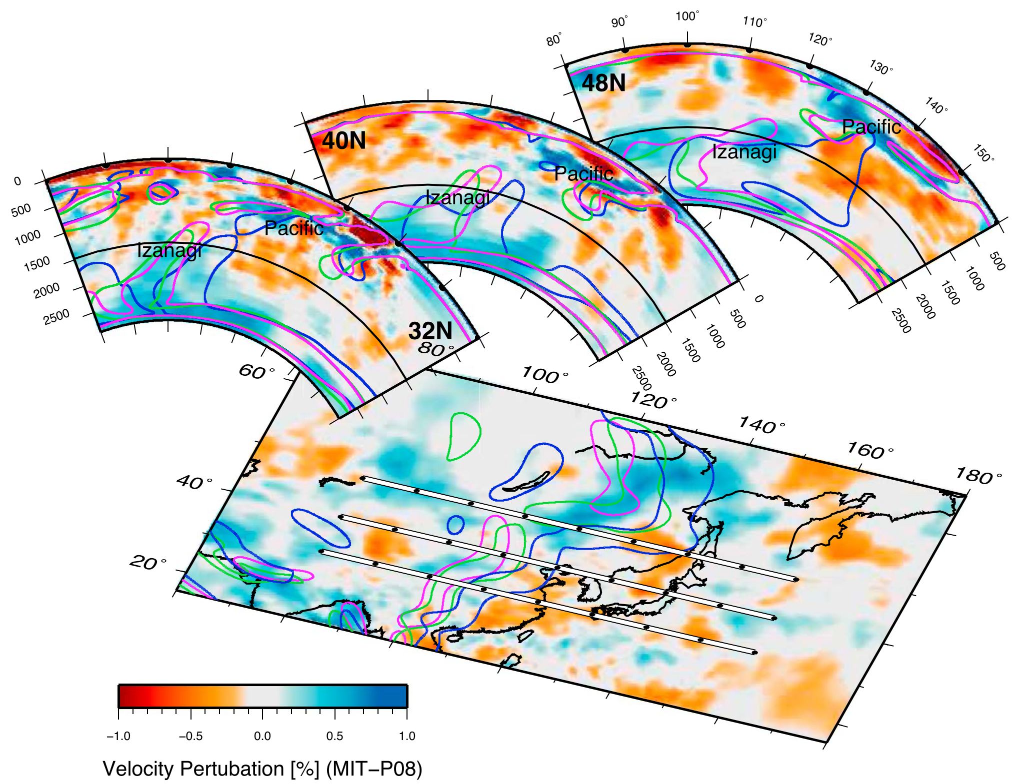

Figure 4. Seismic tomography with geodynamic model output. Perspective view (looking north) of *P* wave seismic tomography [*Li et al*., 2008] at 1445 km depth and along three vertical cross sections at 48°N, 40°N, and 32°N. Magenta contours correspond to model slabs (mantle 10% colder than ambient) from Model 1, green from Model 2, and blue from Model 3. The horizontal black lines on the vertical cross sections denote the depth shown in the map. Pacific = subducted Pacific oceanic lithosphere. Izanagi = subducted Izanagi oceanic lithosphere.

We compare the present-day mantle temperature field predicted by Models 1–3 with seismic tomography, qualitatively (Figures 3, 4 and S1–S3 in the supporting information) and quantitatively (Figure S4). Finally, we examine the evolution of the predicted mantle flow (Figures 3 and 5) to assess whether our tectonic scenario could induce a change in the entire plate-mantle system.

3. Geological Constraints

The intersection of an active mid-ocean ridge with a subduction zone commonly results in the opening of a slab window [*Thorkelson*, 1996]. Typically, the surface manifestations include, but are not limited to cessation of arc volcanism, geochemically distinct magmatism, increased volume and extended range of volcanism, and elevated geothermal gradients and deformation on the overriding plate [*Thorkelson*, 1996]. Geological evidence across Japan, Korea, and China support ridge subduction intersection along East Asia between 55 and 43 Ma (see supporting information Text S1). A detailed structural interpretation of the Shimanto Belt, a Late Cretaceous to Miocene accretionary complex in southeast Japan [*Raimbourg et al*., 2014] (Figure 1), indicates an erosional and extensional phase in the early to middle Eocene consistent with trench-parallel subduction of the Pacific-Izanagi ridge. Additionally, this belt records high levels of thermal maturity within Eocene strata [*Taira et al*., 1988] and a decrease in the age gap between Eocene basaltic rocks and overlying turbidite sediments [*Underwood et al*., 1993]. The trimodal distribution of Andean-type granodioritic batholiths across Japan, Korea, and China [*Nakajima*, 1996; *Sagong et al*., 2005] (Figure 1) indicates a final phase of plutonism in East Asia started 135–100 Ma and continued until about 55–50 Ma [*Nakajima*, 1996; *Sagong et al*., 2005]. Following a hiatus, the system restarted with normal arc magmatism between 43 and 42 Ma [*Nakajima*, 1996; *Sagong et al*., 2005]. This disruption of normal arc magmatic processes is typical for areas above a slab window [*Thorkelson*, 1996].

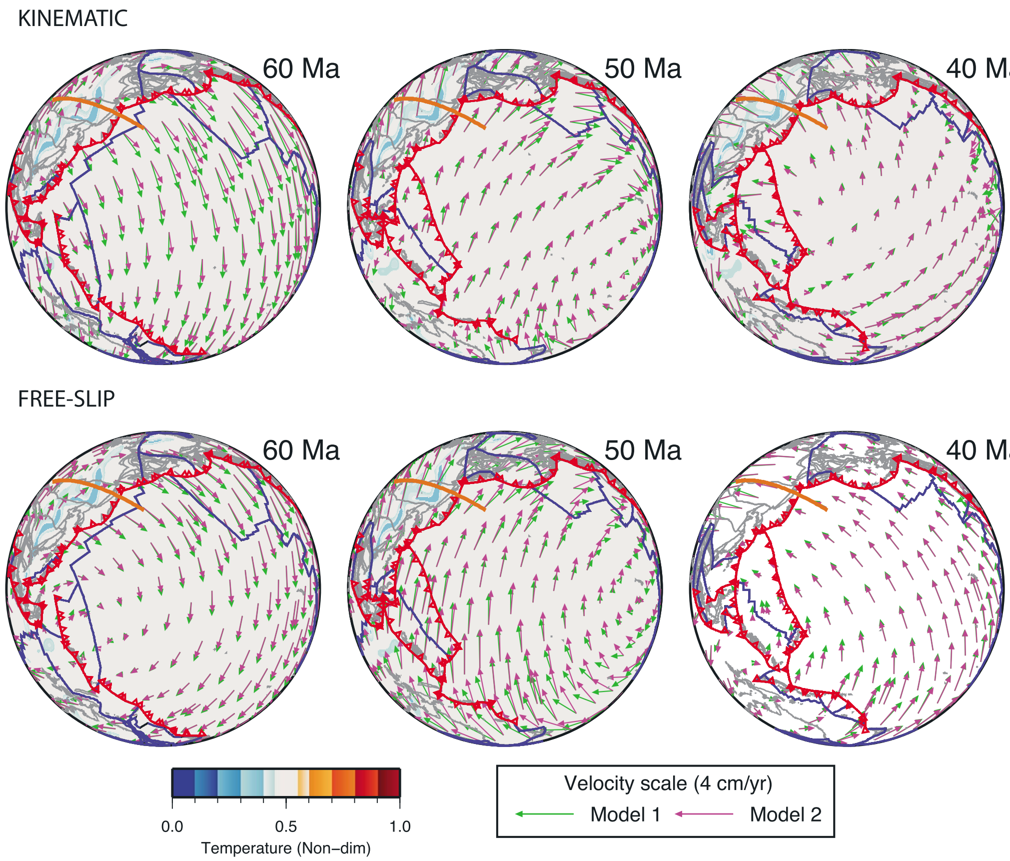

Figure 5. Time-dependent mantle flow field from geodynamic models at 1500 km depth. The lateral mantle flow field from Model 1 (magenta) and Model 2 (green) are shown for each time step, highlighting the change from southward directed mantle flow to the dramatic shift in mantle flow at 50 Ma. (top row) Results with kinematic boundary conditions; (bottom row) results with free-slip boundary conditions. The temperature field is shown for Model 1. Red lines indicate subduction zones, blue indicate transforms and mid-ocean ridges, and the profile plotted in Figure 3 is marked as an orange line.

4. Seismic Tomography and Geodynamic Models

The geodynamic calculations show that the reconstructed plate boundary configuration and plate motions produce a margin-wide slab window and slab detachment associated with the complete subduction of the Izanagi plate beneath East Asia before 50 Ma (Figure 3). The resultant present-day temperature fields reveal a good first-order match with seismic tomography models (Figures 4 and S1–S3), where two distinct structures corresponding to the two major phases of subduction are observed for all three models despite their different viscosity structures. In Model 3 the low-viscosity asthenosphere between 160 and 310 km is offset under the continents using tracers, in order to minimize the net rotation induced to the lower mantle [*Rudolph and Zhong*, 2014]. Indeed, despite the advection of viscous tracers, lower mantle structures are longitudinally shifted in Model 3 that predicts slabs to be ~ 10° farther east in the lower mantle than Models 1 and 2 (Figure 4). Visual inspection reveals that Model 3 does not match tomography as well as Models 1 and 2 (Figures 4 and S1–S3), and we limit further analyses to Models 1 and 2. This result for Model 3 suggests that some net rotation of the lower mantle could have occurred under East Asia since the breakup of Pangea. Slabs are a few tens of kilometers deeper and farther to the west in Model 2 compared to Model 1, which respectively reflects the lesser viscosities in the lower mantle and the absence of an asthenosphere in Model 2.

In all models and tomography, the shallowest slab (Pacific in Figures 4 and S1–S3) reflects the most recent, post 50 Ma westward dipping subduction of Pacific oceanic lithosphere along the Japan-Kuril Trench and corresponds to the shallowest, coldest anomaly in the flow models (Pacific in Figures 4 and S1–S3). We consider the midmantle high-seismic velocity anomaly, located at depths of 1000–2500 km in both geodynamic models and seismic tomography (Izanagi in Figures 4 and S1–S3) to be representative of material subducted prior to the arrival of the Pacific-Izanagi ridge (that is, the subducted Izanagi plate). Although this anomaly has previously been attributed to a middle to late Mesozoic subducted slab [*van der Meer et al*., 2009], our geodynamic models reveal that this material subducted from 110 to 60 Ma (Figure 2), consistent with the final phase of plutonism in Korea [*Sagong et al*., 2005].

We use a simple, quantitative approach to assess the correlation between predicted temperature from our geodynamic models and three *P* wave [*Li et al*., 2008; *Montelli et al*., 2004; *Obayashi et al*., 2013] and one *S* wave [*Grand et al*., 1997] seismic tomography models (Figure S4) by calculating the area of intersecting polygons in both data sets [*Shephard et al*., 2012]. For mantle $\geq$ 10% colder than ambient and positive *P* wave anomalies $\geq$ 0.02% [*van der Meer et al*., 2009], we find that our models produce intersection scores between 70 and 84% for midmantle depths (Figure S4). This suggests the degree of correlation between our model and tomography is good, particularly considering that intersection scores across *P* and *S* wave models themselves for this area are between 50 and 77% (Figure S4). Intersections with tomography are marginally better for Model 1 than for Model 2, making it difficult to find a preferred model.

5. Pacific Midmantle Flow

Coincident with evidence for plate motion changes between 53 and 47 Ma is an indication of a major change in middle to lower mantle flow beneath the Pacific. In order to isolate the contributions of kinematic boundary conditions from flow driven solely by the deeply seated temperature field, we investigate sub-Pacific midmantle flow for kinematic and free-slip boundary conditions (Figure 5). For both sets of boundary conditions, a major mantle flow pattern reorganization occurs between 60 and 50 Ma (Figures 3 and 5). Flow directions are broadly consistent between both models, and small differences in azimuth and amplitude reflect different viscosity structures between models.

Prior to the reorganization (60 Ma), our calculations show a southward directed midmantle lateral flow beneath the Pacific plate (Figure 5) at a rate of between 0.5 and 1.7 cm/yr (0.1–1.2 cm/yr for free-slip boundary conditions). A contribution to this lateral flow under the northwest Pacific may be due to return flow from the coherent slab structures along the East Asian margin. This is followed by a major shift in the direction of mantle flow toward the north and northeast at 50 Ma, which may be related to a weakening of the return flow after ridge subduction and slab break off. This major shift in mantle flow indicates the onset of a reorganization of the Pacific mantle and is accompanied by a slight decrease in mantle flow rate to a maximum of 1.4 cm/yr (Figure 5) (1.4 cm/yr for free-slip boundary conditions). The reorganization of Pacific mantle flow was likely complete by 40 Ma with a return to slower, north to northwest directed flow of between 0.1 and 1.1 cm/yr (0.4–1.2 cm/yr for free-slip boundary conditions) (Figures 3 and 5). Interestingly, our mantle flow velocities prior to 50 Ma are consistent with the southward directed mantle flow implied by studies of the motion of the Hawaiian hot spot [*Tarduno et al*., 2009].

6. Discussion

Numerical models designed to investigate the effects of the complete subduction of an oceanic plate indicate that the arrival of a mid-ocean ridge at the trench is preceded by slab detachment, due to a reduction in strength and negative buoyancy of approaching oceanic lithosphere and the loss of transmission of slab pull force to the surface [*Burkett and Billen*, 2009]. The clear break in structure evident in seismic tomographic images under eastern Eurasia at depths between 500 and 1000 km (Figure 4) and replicated at similar depths in models (Figure 3) reflects slab detachment and short-lived quiescence in subduction associated with the subparallel arrival of the Pacific-Izanagi ridge to the East Asian margin between 60 and 50 Ma. In our calculations, the formation of the gap in the continuity of the slab occurred between 60 and 40 Ma (Figure 3). A decrease in slab pull force would be expected to result in a major change in the rate and direction of plate motion [*Stadler et al*., 2010], characteristic of plate reorganizations [*Conrad et al*., 2004]. In the case of East Asia, the margin-wide slab detachment would have led to a marked change in the forces acting on the Pacific plate, from being surrounded by mid-ocean ridges prior to 55–50 Ma to the establishment of a major subduction system along its western boundary. Indeed, a study of the slab pull acting on the Pacific plate before, during, and after 50 Ma [*Faccenna et al*., 2012] support a change that increases a slab pull westward after 50 Ma.

We suggest that the subparallel arrival of the Izanagi-Pacific ridge to the East Asian subduction zone 55–50 Ma led to a cascade of events that culminated in a reorganization of Pacific mantle flow, triggering tectonic changes around the Pacific Ocean basin. Slab detachment and slab window formation resulted in a change in plate-driving forces acting along the western Pacific due to the progressive decrease in buoyancy of the downgoing plate and eventual loss of slab pull. The overall change in the forces on the Pacific plate may have led to a change of stress on the nascent boundary [*Leng and Gurnis*, 2011] between the Pacific and West Philippine plates that initiated subduction along the Izu-Bonin-Mariana margin at 52 Ma [*Ishizuka et al*., 2011]. We suggest that the rapid reorganization of Pacific midmantle lateral flow between 60 and 50 Ma, replicated in our models, was a consequence of surface plate motion changes, consistent with the hypothesis that the reorganization of the Pacific plate-mantle system was a plate tectonically driven, mantle-scale process. The reorganization, which occurred over a period of ~7 Myr (between ~53 and 47 Ma), is consistent with the timing of tectonic events throughout the Pacific hemisphere around this time. This scenario should be testable with new generation of high-resolution, fully dynamic, global models, particularly in assessing the geodynamic processes associated with ridge-trench intersection events.

Acknowledgments
This study was supported by Australian Research Council grants DP0987713 (M.S.), FL0992245 (R.D.M.), and DE14100376 (J.W.); Statoil ASA industry research grants through ARC IH130200012; and partial support by the National Science Foundation EAR-1247022 and CMMI-1028978 (D.J.B. and M.G.). This research was undertaken with the assistance of resources provided at the NCI National Facility through the National Computational Merit Allocation Scheme supported by the Australian Government. We thank Thomas Landgrebe for his assistance with calculating intersection scores.

The Editor thanks Lijun Liu and an anonymous reviewer for their assistance in evaluating this paper.

References

Bloomer, S. H., B. Taylor, C. J. MacLeod, R. J. Stern, P. Fryer, J. W. Hawkins, and L. Johnson (1995), Early arc volcanism and the ophiolite problem: A perspective from drilling in the western Pacific, in *Active Margins and Marginal Basins of the Western Pacific*, vol. 88, edited by B. Taylor and J. Natland, pp. 1–30, AGU, Washington, D. C.

Bower, D. J., M. Gurnis, and N. Flament (2015), Assimilating lithosphere and slab history in 4-D Earth models, *Phys. Earth Planet. Inter.*, *238*, 8–22.

Boyden, J. A., R. D. Müller, M. Gurnis, T. H. Torsvik, J. A. Clark, M. Turner, H. Ivey-Law, R. J. Watson, and J. S. Cannon (2011), Next-generation plate-tectonic reconstructions using GPlates, in *Geoinformatics: Cyberinfrastructure for the Solid Earth Sciences*, edited by G. R. Keller and C. Baru, pp. 95–114, Cambridge Univ. Press, Cambridge.

Burkett, E. R., and M. I. Billen (2009), Dynamics and implications of slab detachment due to ridge-trench collision, *J. Geophys. Res.*, *114*, B12402, doi:10.1029/2009JB006402.

Cande, S. C., and D. R. Stegman (2011), Indian and African plate motions driven by the push force of the Reunion plume head, *Nature*, *475*(7354), 47–52.

Cande, S. C., E. M. Herron, and B. R. Hall (1982), The early Cenozoic tectonic history of the southeast Pacific, *Earth Planet. Sci. Lett.*, *57*(1), 63–74.

Caress, D. W., H. W. Menard, and R. N. Hey (1988), Eocene reorganization of the Pacific-Farallon Spreading Center north of the Mendocino Fracture Zone, *J. Geophys. Res.*, *93*, 2813–2838, doi:10.1029/JB093iB04p02813.

Conrad, C. P., S. Bilek, and C. Lithgow-Bertelloni (2004), Great earthquakes and slab pull: Interaction between seismic coupling and plate-slab coupling, *Earth Planet. Sci. Lett.*, *218*(1–2), 109–122.

Faccenna, C., T. Becker, S. Lallemand, and B. Steinberger (2012), On the role of slab pull in the Cenozoic motion of the Pacific, *Geophys. Res. Lett*, *39*, L03305, doi:10.1029/2011GL050155.

Finn, C. A., R. D. Müller, and K. S. Panter (2005), A Cenozoic diffuse alkaline magmatic province (DAMP) in the southwest Pacific without rift or plume origin, *Geochem. Geophys. Geosyst.*, *6*, Q02005, doi:10.1029/2004GC000723.

Flament, N., M. Gurnis, S. Williams, M. Seton, J. Skogseid, C. Heine, and R. Dietmar Müller (2014), Topographic asymmetry of the South Atlantic from global models of mantle flow and lithospheric stretching, *Earth Planet. Sci. Lett.*, *387*, 107–119.

Gaina, C., D. R. Müller, J. Y. Royer, J. Stock, J. Hardebeck, and P. Symonds (1998), The tectonic history of the Tasman Sea: A puzzle with 13 pieces, *J. Geophys. Res.*, *103*, 12,413–12,433, doi:10.1029/98JB00386.

Goes, S., F. A. Capitanio, and G. Morra (2008), Evidence of lower-mantle slab penetration phases in plate motions, *Nature*, *451*(7181), 981–984.

Grand, S. P., R. D. van der Hilst, and S. Widiayantoro (1997), Global seismic tomography: A snapshort of convection in the Earth, *GSA Today*, *4*, 1–7.

Gurnis, M., M. Turner, S. Zahirovic, L. DiCaprio, S. Spasojevic, R. Müller, J. Boyden, M. Seton, V. Manea, and D. Bower (2012), Plate tectonic reconstructions with continuously closing plates, *C. R. Geosci.*, *38*, 35–42.

Ishizuka, O., K. Tani, M. K. Reagan, K. Kanayama, S. Umino, Y. Harigane, I. Sakamoto, Y. Miyajima, M. Yuasa, and D. J. Dunkley (2011), The timescales of subduction initiation and subsequent evolution of an oceanic island arc, *Earth Planet. Sci. Lett.*, *306*(3), 229–240.

Leng, W., and M. Gurnis (2011), Dynamics of subduction initiation with different evolutionary pathways, *Geochem. Geophys. Geosyst.*, *12*, Q12018, doi:10.1029/2011GC003877.

Li, C., R. van der Hilst, E. Engdahl, and S. Burdick (2008), A new global model for *P* wave speed variations in Earth's mantle, *Geochem. Geophys. Geosyst*, *9*, Q05018, doi:10.1029/2007GC001806.

Lonsdale, P. (1988), Paleogene history of the Kula plate: Offshore evidence and onshore implications, *Geol. Soc. Am. Bull.*, *100*(5), 733.

Matthews, K. J., R. D. Müller, P. Wessel, and J. M. Whittaker (2011), The tectonic fabric of the ocean basins, *J. Geophys. Res.*, *116*, B12109, doi:10.1029/2011JB008413.

Molnar, P., and P. Tapponnier (1975), Cenozoic tectonics of Asia: Effects of a continental collision, *Science*, *189*(4201), 419–426.

Montelli, R., G. Nolet, F. Dahlen, G. Masters, E. R. Engdahl, and S.-H. Hung (2004), Finite-frequency tomography reveals a variety of plumes in the mantle, *Science*, *303*(5656), 338–343.

Müller, R. D., W. R. Roest, and J.-Y. Royer (1998), Asymmetric sea-floor spreading caused by ridge–plume interactions, *Nature*, *396*(6710), 455–459.

Nakajima, T. (1996), Cretaceous granitoids in SW Japan and their bearing on the crust-forming process in the eastern Eurasian margin, *Geol. Soc. Am. Spec. Pap.*, *315*, 183.

Obayashi, M., J. Yoshimitsu, G. Nolet, Y. Fukao, H. Shiobara, H. Sugioka, H. Miyamachi, and Y. Gao (2013), Finite frequency whole mantle *P* wave tomography: Improvement of subducted slab images, *Geophys. Res. Lett.*, *40*, 5652–5657, doi:10.1002/2013GL057401.

O'Connor, J. M., B. Steinberger, M. Regelous, A. A. Koppers, J. R. Wijbrans, K. M. Haase, P. Stoffers, W. Jokat, and D. Garbe-Schönberg (2013), Constraints on past plate and mantle motion from new ages for the Hawaiian-Emperor Seamount Chain, *Geochem. Geophys. Geosyst.*, *14*, 4564–4584, doi:10.1002/ggge.20267.

Patriat, P., and J. Achache (1984), India–Eurasia collision chronology has implications for crustal shortening and driving mechanism of plates, *Nature*, *311*(5987), 615–621, doi:10.1038/311615a0.

Raimbourg, H., R. Augier, V. Famin, L. Gadenne, G. Palazzin, A. Yamaguchi, and G. Kimura (2014), Long-term evolution of an accretionary prism: The case study of the Shimanto Belt, Kyushu, Japan, *Tectonics*, *33*, 936–959, doi:10.1002/2013TC003412.

Rudolph, M., and S. Zhong (2014), History and dynamics of net rotation of the mantle and lithosphere, *Geochem. Geophys. Geosyst.*, *15*, 3645–3657, doi:10.1002/2014GC005457.

Sagong, H., S. Kwon, and J. Ree (2005), Mesozoic episodic magmatism in South Korea and its tectonic implication, *Tectonics*, *24*, TC5002, doi:10.1029/2004TC001720.

Seton, M., et al. (2012), Global continental and ocean basin reconstructions since 200 Ma, *Earth Sci. Rev.*, *113*(3–4), 212–270.

Sharp, W. D., and D. A. Clague (2006), 50-Ma initiation of Hawaiian-Emperor bend records major change in Pacific Plate motion, *Science*, *313*(5791), 1281–1284.

Shephard, G. E., H.-P. Bunge, B. S. Schuberth, R. Müller, A. Talsma, C. Moder, and T. Landgrebe (2012), Testing absolute plate reference frames and the implications for the generation of geodynamic mantle heterogeneity structure, *Earth Planet. Sci. Lett.*, *317*, 204–217.

Stadler, G., M. Gurnis, C. Burstedde, L. C. Wilcox, L. Alisic, and O. Ghattas (2010), The dynamics of plate tectonics and mantle flow: From local to global scales, *Science*, *329*(5995), 1033–1038.

Stern, R. J. (2004), Subduction initiation: Spontaneous and induced, *Earth Planet. Sci. Lett.*, *226*(3–4), 275–292.

Straub, S., S. Goldstein, C. Class, and A. Schmidt (2009), Mid-ocean-ridge basalt of Indian type in the northwest Pacific Ocean basin, *Nat. Geosci.*, *2*(4), 286–289.

Taira, A., J. Katto, M. Tashiro, M. Okamura, and K. Kodama (1988), The Shimanto belt in Shikoku, Japan ,evolution of Cretaceous to Miocene accretionary prism, *Mod. Geol.*, *12*(5), 46.

Tan, E., W. Leng, S. Zhong, and M. Gurnis (2007), CitcomS v3.0—A compressible thermo-chemical mantle convection code.

Tarduno, J., H. Bunge, N. Sleep, and U. Hansen (2009), The bent Hawaiian-Emperor hotspot track: Inheriting the mantle wind, *Science*, *324*(5923), 50.

Thorkelson, D. J. (1996), Subduction of diverging plates and the principles of slab window formation, *Tectonophysics*, *255*(1–2), 47–63.

Underwood, M. B., J. Hibbard, and L. DiTullio (1993), Geologic summary and conceptual framework for the study of thermal maturity within the Eocene-Miocene Shimanto Belt, Shikoku, Japan, *Spec. Pap. Geol. Soc. Am.*, *273*, 1–24.

van der Meer, D., W. Spakman, D. van Hinsbergen, M. Amaru, and T. Torsvik (2009), Towards absolute plate motions constrained by lower-mantle slab remnants, *Nat. Geosci.*, *3*, 36–40, doi:10.1038/ngeo708.

Whittaker, J., R. D. Müller, G. Leitchenkov, H. Stagg, M. Sdrolias, C. Gaina, and A. Goncharov (2007), Major Australian-Antarctica Plate reorganization at Hawaiian-Emperor Bend Time, *Science*, *318*, 83–86.

